ELSEVIER

www.elsevier.nl/locate/jorganchem

Journal of Organometallic Chemistry 587 (1999) 233–243

Journal of Organo metallic Chemistry

# Interplay of ketenyl and nitrile ligands on $d^6$-transition metal centres. Acetonitrile as an end-on (two-electron) and a side-on (four-electron) ligand

Hubert Wadepohl [a,*], Ulrich Arnold [a], Hans Pritzkow [a], Maria José Calhorda [b,1], Luís F. Veiros [c]

[a] *Anorganisch-Chemisches Institut der Ruprecht-Karls-Universität, Im Neuenheimer Feld 270, D-69120 Heidelberg, Germany*
[b] *ITQB, Quinta do Marquês, EAN, Apart. 127, 2781-901 Oeiras, Portugal and Departamento de Química e Bioquímica, Faculdade de Ciências, Universidade de Lisboa, 1749-016 Lisbon, Portugal*
[c] *CQE, Instituto Superior Técnico, Av. Rovisco Pais, 1096 Lisbon Codex, Portugal*

Received 12 March 1999; received in revised form 9 April 1999

Dedicated to Professor Dirk Walther on the occasion of his 60th birthday.

---

## Abstract

Carbyne carbonyl coupling takes place in acetonitrile solutions of the Fischer-type carbyne complexes $[tpb'(CO)_2Mo{\equiv}CC_6H_4Me\text{-}4]$ (**4b**) (tpb′ = tris(3,5-dimethylpyrazolyl)hydroborate) and $[(C_5Me_5)(CO)_2W{\equiv}CSiPh_3]$ (**5**). The product $[tpb'(CO)(NCMe)Mo\{C(C_6H_4Me\text{-}4)CO\}]$ (**7b**) has conventional $\eta^1$-nitrile and $\eta^2$-ketenyl ligands. In contrast, the product $[(C_5Me_5)(CO)(NCMe)W\{C(SiPh_3)CO\}]$ (**8**) displays a highly unusual 'four-electron-donor' $\eta^2$-nitrile and a $\eta^1$-ketenyl ligand. The structures of **4b**, $[tpb'(CO)_2W{\equiv}CC_6H_4Me\text{-}4]$ **6**, **7b** and **8** were determined by X-ray crystallography. Extended Hückel and density functional theory (DFT) calculations on model compounds show that the observed coordination geometry around W is the electronically preferred for **8**. The side-on nitrile in this and other related complexes binds to the metal donating from the two highest occupied orbitals (corresponding to the nitrogen lone pair and the $\pi_\perp$), in contrast to two-electron donors where only the HOMO is involved in bonding. Back-donation takes place for all the side-on bound nitriles. © 1999 Elsevier Science S.A. All rights reserved.

*Keywords:* Ketenyl; Nitrile; $d^6$-Transition metal centers

---

## 1. Introduction

Coupling of an alkylidyne and a carbonyl ligand is a general reactivity pattern for low-valent (especially Fischer-type) metal carbyne complexes. This reaction was first reported in 1976 by Kreißl et al., who obtained the $\eta^1$-ketenyl complex **3** (M = W, R = *p*-tolyl) when tolylcarbyne cyclopentadienyl dicarbonyltungsten **1** (M = W, R = *p*-tolyl) was treated with two equivalents of $PMe_3$ [1]. Subsequently, it was shown by the same group that formation of the $\eta^1$-ketenyl complexes **3** proceeds via the $\eta^2$-ketenyl complexes **2** [2]. In the following years more examples of alkylidyne carbonyl coupling reactions have been discovered, not only induced by nucleophiles (such as $PMe_3$) but also by electrophiles or photons [3,4]. The structures and reactions of ketenyl complexes have been reviewed [5].

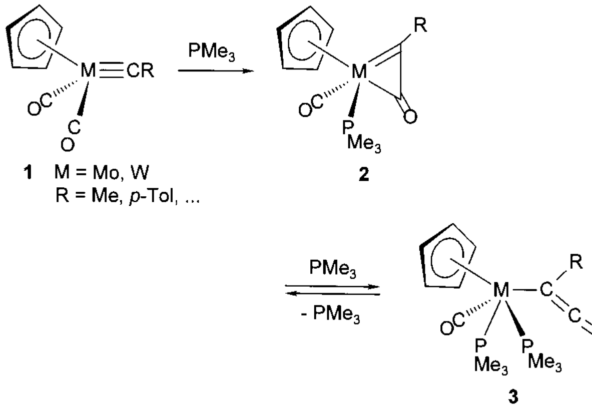

---

* Corresponding author. Tel.: +49-6221-54-4827; fax: +49-6221-54-4197.

*E-mail address:* bu9@ix.urz.uni-heidelberg.de (H. Wadepohl)

[1] Also corresponding author.

PII: S0022-328X(99)00328-9

In the course of our studies of the hydroboration of metal carbon multiple bonds we discovered that during the reactions of the Fischer-type metal carbyne complexes $[X(CO)_2M{\equiv}CR]$ ($X = C_5H_5$, $C_5Me_5$, tpb, tpb′; M = Mo, W) [tpb = tris(pyrazolyl)hydroborate, tpb′ = tris(3,5-dimethylpyrazolyl)hydroborate] with hydroboranes different reaction pathways are followed, depending on the nature of X [6]. These observations prompted a more general study of the alkylidyne reactivity of some derivatives $[X(CO)_2M{\equiv}R]$ with strongly electron donating ligands X. Here we wish to report the differing structures of the products that resulted from the intramolecular carbyne–carbonyl coupling induced by acetonitrile in the complexes $[tpb'(CO)_2Mo{\equiv}CC_6H_4Me\text{-}4]$ (**4b**) and $[(C_5Me_5)(CO)_2W{\equiv}CSiPh_3]$ (**5**).

## 2. Results and discussion

### 2.1. *Tris(dimethylpyrazolyl)borate complexes*

A number of carbyne complexes with the $tpb'(CO)_2(d^6\text{-}M)$ fragment have been reported, including the phenylcarbyne molybdenum **4a** [7,9] and *p*-tolylcarbyne tungsten **6** [8] derivatives. Using a modification of the procedure published for **6**, we prepared the new complex **4b** in 57% yield from $[Br(CO)_4Mo{\equiv}CC_6H_4Me\text{-}4]$ and K(tpb′). The IR ($\nu_{CO}$) and NMR spectroscopic data of **4b** closely resemble the published data for **6**. When a saturated acetonitrile solution of **4b** was kept in the daylight, a colour change from orange–red to dark-green took place. After about 4 days, quantitative conversion of **4b** into the ketenyl complex **7b** was observed. Such a carbyne–carbonyl coupling reaction to give **7a** had previously been observed with the phenylcarbyne derivative **4a** upon irradiation with Pyrex-filtered UV light [9]. Under similar conditions, the tungsten complex **6** did not undergo this reaction. It had been noted earlier that the tris(pyrazolyl) derivative of **6**, $[tpb(CO)_2W{\equiv}CC_6H_4Me\text{-}4]$, while reacting with $PMe_3$ to afford the ketenyl complex $[tpb(CO)(PMe_3)W\{\eta^2\text{-}C(p\text{-tolyl})C{=}O\}]$ [10] did not give an analogous product with the less nucleophilic $PPh_3$ [11].

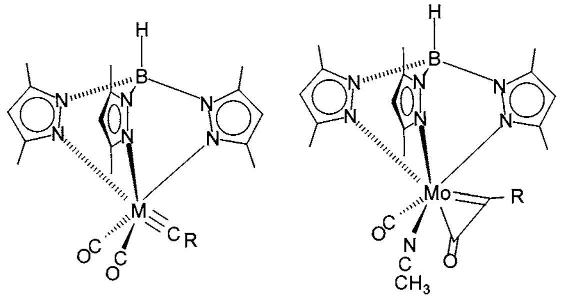

**4a** M = Mo, R = Ph
**4b** M = Mo, R = *p*-Tol
**6** M = W, R = *p*-Tol

**7a** R = Ph
**7b** R = *p*-Tol

As expected, the spectroscopic data of **7b** are very similar to those of **7a** and need not be discussed here. Single crystals of **4b**·MeCN and **7b**·MeCN were obtained by fractional crystallisation of the reaction mixtures before conversion was complete. Crystals of **6**·MeCN were grown from acetonitrile at −20°C.

The crystal structures of **4b**·MeCN and of **6**·MeCN are isotypic. In both cases one molecule of acetonitrile is present in the asymmetric unit as a solvent of crys-

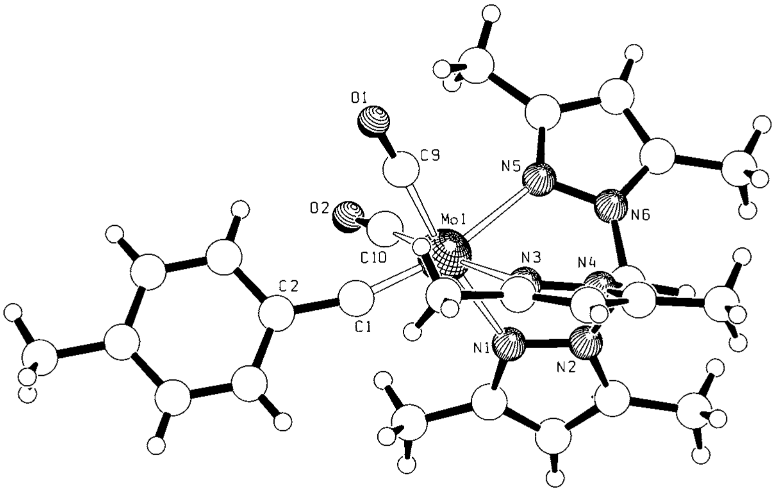

Fig. 1. Molecular structure of $[tpb'(CO)_2Mo{\equiv}CC_6H_4Me\text{-}4]$ (**4b**). Important bond distances (Å) and angles (°) with estimated S.D. in parentheses: **4b**: Mo1–C1 1.804(4), Mo1–C9 1.987(4), Mo1–C10 1.987(4), Mo1–N1 2.218(3), Mo1–N3 2.212(3), Mo1–N5 2.306(3), C1–C2 1.449(5), C9–O1 1.145(5), C10–O2 1.140(5); Mo1–C1–C2 163.1(3), Mo1–C9–O1 176.9(4), Mo1–C10–O2 176.3(4). **6**: W1–C1 1.829(3), W1–C9 1.985(4), W1–C10 1.994(4), W1–N1 2.210(3), W1–N3 2.288(3), W1–N5 2.203(3), C1–C2 1.448(4), C9–O1 1.159(5), C10–O2 1.146(5); W1–C1–C2 163.2(3), W1–C9–O1 177.6(4), W1–C10–O2 176.3(4).

tallisation. The molecular structure of **4b** is shown in Fig. 1.

The structural parameters of **4b** and **6** are quite similar, with only minor deviations caused by the two different metals. The distances between the metal atoms and the carbyne carbons, 1.80 Å (**4b**) and 1.83 Å (**6**), fall within the usual range [12]. The carbyne fragments are noticeably nonlinear on C1 (angle, metal–C1–C2 163°). This is different from carbyne complexes with the isoelectronic $(C_5R_5)(CO)_2M$ fragment, where linear carbynes are generally found [12]. In view of a similar distortion in $[\{(pz)_4B\}(CO)_2W{\equiv}CC_6H_4Me\text{-}4]$ [10] with the less bulky tetrakis(pyrazolyl)borate $[(pz)_4B]$ ligand, a steric cause for the observed deviation from linearity is unlikely. A strong *trans* influence of the carbyne ligands is evident in the lengthening of the metal–nitrogen bond *trans* to C1 (2.31 Å versus 2.21, 2.22 Å).

The linear acetonitrile molecules are situated in pairs (with an antiparallel orientation, related by a centre of symmetry) between the metal carbyne molecules. They do not show any unusually short intermolecular contacts. The nitrile N–C distances (1.112(7), 1.125(7) Å) are close to that in free acetonitrile [13,14].

The carbyne–carbonyl coupling product **7b** also crystallises as an acetonitrile solvate. The molecular structure of the ketenyl complex is shown in Fig. 2.

The *p*-tolyl substituted ketenyl ligand in **7b** adopts the $\eta^2$ coordination mode to the molybdenum atom. The CC and CO bond lengths within the $\eta^2$-C(R)C=O unit are similar to those of the few other structurally characterised $\eta^2$-ketenyl complexes [2a,11,15,16,17,18]; they are somewhat lengthened with respect to free ketene [19]. The nonlinear ketenyl ligand resembles an $\eta^2$-alkyne. The orientation of this ligand with respect to rotation around the bond axis to the metal is such that the ketenyl–CO group is placed adjacent to the carbonyl ligand C26O2. This is in accord with earlier theoretical calculations [20] and with the geometry of the other known examples [3].

Of the two linear acetonitrile molecules in the asymmetric unit one is $\eta^1$-bonded to the molybdenum centre via its nitrogen atom. The other nitrile packs in between the molecules of **7b** as a solvent of crystallisation. Coordination of the nitrile to the metal results in a lengthening of the NC bond by about 0.03 Å. The bond distances between the molybdenum atom and the pyrazolyl nitrogens fall in two groups, a shorter bond *trans* to the nitrile ligand (2.17 Å) and two longer ones *trans* to carbon monoxide (2.26 Å) and the $\eta^2$-ketenyl ligand (2.27 Å), respectively. Hence, a much larger *trans* influence can be assigned to the two latter ligands.

### 2.2. Pentamethylcyclopentadienyl complex

When treated with acetonitrile at −20°C and then warmed to room temperature (r.t.), the tungsten triphenylsilyl carbyne complex **5** also undergoes carbyne–carbonyl coupling, to give the ketenyl complex **8**. However, the coupling reaction is much more easily reversible here, and **8** can only be obtained pure in the crystalline solid state. Dissolved in methylene chloride or benzene **8** slowly splits off the nitrile ligand to give a green equilibrium mixture of orange–yellow **5** and blue **8**.

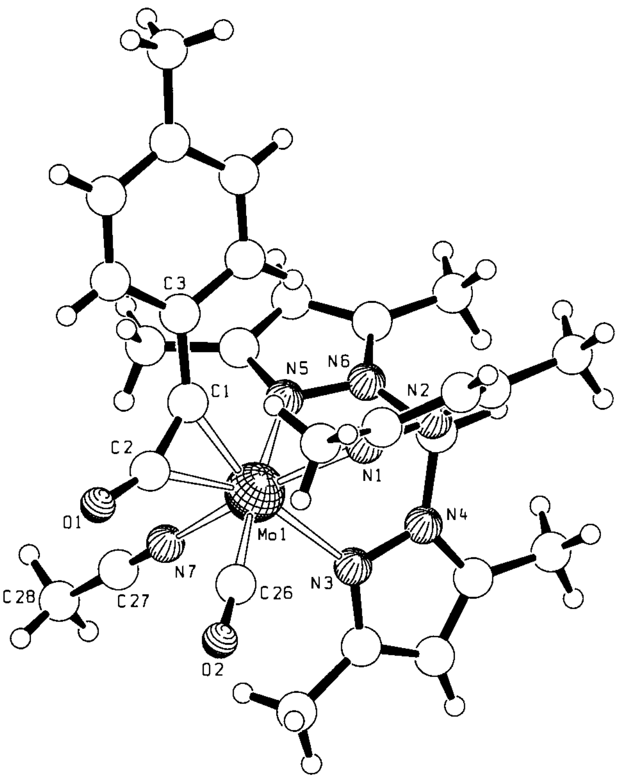

Fig. 2. Molecular structure of $[tpb'(CO)(NCMe)Mo\{C(C_6H_4Me\text{-}4){=}C{=}O\}]$ (**7b**). Important bond distances (Å) and angles (°) with estimated S.D. in parentheses: Mo1–C1 2.002(4), Mo1–C2 2.210(4), Mo1–C26 1.917(5), Mo1–N1 2.173(4), Mo1–N3 2.270(4), Mo1–N5 2.262 (4), Mo1–N7 2.159(4), C1–C2 1.361(6), C1–C3 1.451(6), C2–O1 1.194(6), C26–O2 1.185(6), N7–C27 1.137(6), C27–C28 1.444(7); C3–C1–C2 134.3(4), C1–C2–O1 153.2(5), Mo1–C26–O2 176.6(4), Mo1–N7–C27 179.0(4), N7–C27–C28 178.6(6).

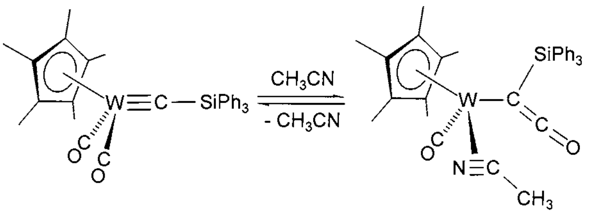

**5** **8**

The crystal structure analysis of complex **8** reveals coordination modes of the nitrile and ketenyl ligands which are quite different from those in **7b** (Fig. 3).

The $Ph_3Si$-substituted ketenyl ligand binds to the tungsten atom via its carbon atom C1 only. Compared to the $\eta^2$-ketenyl in **7b**, the bond angles around C1 more closely approach the value (120°) expected from $sp^2$-hybridisation. Despite the somewhat acute angle W1–C1–C2 (105.2°), the linearity of the C1=C2=O1 unit and the long distance W1···C2 of 2.808 Å rule out a significant interaction of the metal atom with C2.

The nonlinear (136°) acetonitrile ligand is bonded to the tungsten atom in a side-on ($\eta^2$) fashion. The coordination geometry, notably the short W1–N1 and W1–C4 distances and the long bond N1–C4, indicates that this ligand should be considered a four-electron donor, as required for an 18 valence electron configuration of the tungsten atom.

Although a number of examples have been reported [21], the side-on coordination mode is quite unusual for a nitrile. Even more, unlike the ubiquitous 'four-electron-donor' alkyne ligands [22], $\eta^2$-coordinated nitriles only very rarely serve as four-electron donors. To our knowledge, this property has hitherto been established in only a few complexes, which are collected in the first section of Table 1. The second part contains another nitrile complex, **15**, where this ligand has been proposed to be a three-electron donor. The last section contains a few examples of unequivocal side-on bound two-electron-donor nitrile complexes, well characterised by X-ray diffraction. The most relevant features of all complexes are given in the table.

The acetonitrile ligand in **8** displays some of the characteristics of the tungsten phosphine complexes **10**–**13**, notably the above-mentioned short W–N and W–C bonds as well as the long nitrile N–C distances. The metal–nitrogen bond is shorter than the metal–carbon bond. The data relative to other side-on bound nitrile complexes in Table 1 show a tendency for longer M–C and M–N bonds, as well as shorter N–C bonds in the 2e-donor ligands. The so-called three-electron donor nitrile complex **15** is, from a structural point of view, more similar to the two-electron donors than to the four-electron donors.

A correlation has been proposed between the electron donor properties of alkyne ligands and their $^{13}$C-NMR chemical shifts [22]. There are fairly well separated regions on the $\delta$ scale for alkynes formally functioning as two, three or four-electron donors, the latter resonating at the lowest field (highest $\delta$). Although much less data are available, a similar behaviour for the carbon resonances of side-on coordinated nitriles appears evident (Table 1). For **8**, the corresponding resonance ($\delta = 203.4$) is consistent with a four-electron-donor nitrile. $\eta^1$-Ketenyl ligands usually show the $^{13}$C(=O) resonance in the low-field region of the spectrum around $\delta = 150\ldots170$, and a high-field signal ($\delta = 10\ldots-30$) for the metal-bound carbon atom [2,16]. Carbon resonances due to the ketenyl ligand in **8** are observed at $\delta = 169.3$ and 20.7. In the related $\eta^1$-ketenyl complex $[(C_5H_5)(CO)_2(PMe_3)W\{C(SiPh_3)CO\}]$ a signal was found for the metal-bound ketenyl carbon at a considerably higher field, $\delta = -49.7$ [2c]. During the discussion of the

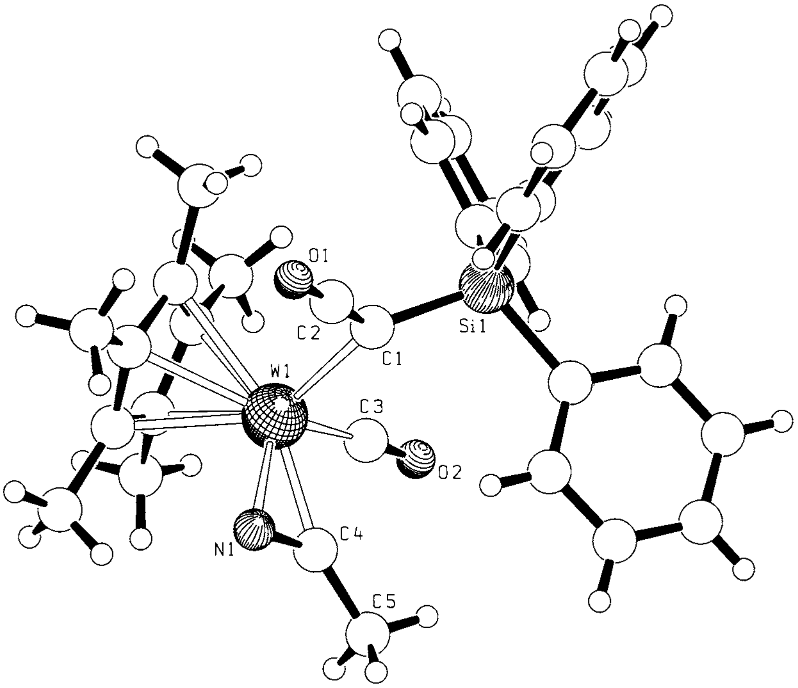

Fig. 3. Molecular structure of $[(C_5Me_5)(CO)(NCMe)W\{C(SiPh_3)=C=O\}]$ (**8**). Important distances (Å) and angles (°) with estimated S.D. in parentheses: W1–C1 2.174(3), W1–C3 1.942(4), W1–C4 2.058(4), W1–N1 2.020(3), W1–C($C_5Me_5$) 2.295(4)–2.446(4), C1–C2 1.296(5), C1–Si1 1.848(4), C2–O1 1.180(5), C3–O2 1.165(5), C4–N1 1.257(5), C4–C5 1.487(5); C2–C1–Si1 123.4(3), W1–C1–C2 105.2(3), W1–C1–Si1 123.4(3), C1–C2–O1 178.5(4), W1–C3–O2 174.7(3), N1–C4–C5 136.1(4).

Table 1
Structural data of side-on bound nitrile complexes

| Complex | M–C (Å) | M–N (Å) | N–C (°) | N–C–C (°) | $\delta(^{13}C)$ | Ref. |
|---|---|---|---|---|---|---|
| Four-electron donors | | | | | | |
| $[W(C_5Me_5)(CO)(MeCN)\{C(SiPh_3)CO\}]$ (**8**) | 2.058(4) | 2.020(3) | 1.257(5) | 136 | 203 | This work |
| $[Mo(dmpe)_2Cl(MECN)][BPh_4]$ (**9**) | 1.981(7) | 1.959(7) | 1.217(8) | 130 | [a] | [21e] |
| $[W(bipy)(PMe_3)_2Cl(MeCN)][PF_6]$ (**10**) | 1.998(5) | 2.008(4) | 1.267(7) | 130 | 235 | [21f] |
| $[W(PMe_3)_3Cl_2(MECN)]$ (**11**) | 1.98(1) | 1.99(1) | 1.27(2) | 129 | 230 | [21g] |
| $[W(NMe\text{–}Paa)(CO)F(C_5F_5CN)]$ (**12**) | 2.009(6) | 1.995(5) | 1.262(7) | 132 | 225 | [21j] |
| $[W(NMe\text{–}Paa)(CO)F(NCC_6F_4CN)]$ (**13**) | 2.039(9) | 2.035(8) | 1.28(1) | 130 | 226 | [21j] |
| $[W(tpb')(CO)(S_2PR_2)(MECN)]$ (**14**) | 2.051(7) | 2.033(6) | 1.225(9) | 138 | 202–204 | [21h,k] |
| Three-electron donors | | | | | | |
| $[Nb(tpb')(CO)(PhCCMe)(C_6H_5CN)]$ (**15**) | 2.17(1) | 2.139(8) | 1.21(1) | 135 | 174–187 | [21i] |
| Two-electron donors | | | | | | |
| $[Mo(C_5H_5)_2(MeCN)]$ (**16**) | 2.124(8) | 2.219(7) | 1.20(1) | 139 | 171 | [21b] |
| $[Ir(C_5H_5)(PPh_3)(p\text{-}ClC_6H_4CN)]$ (**17**) | 2.105(23) | 2.174(15) | 1.231(28) | [a] | [a] | [21c] |
| $[Ir(C_5Me_5)(CO)(p\text{-}ClC_6H_4CN)]$ (**18**) | 2.040(8) | 2.185(5) | 1.209(11) | [a] | [a] | [21c] |

[a] Not reported.

structure of $[(C_5H_5)(CO)(Et_3NC{\equiv}CMe)W\{C(p\text{-tolyl})CO\}]$ (**19**), where an electron-rich alkyne plays the role of the nitrile ligand of **8**, Kreißl et al. pointed out the significance of a possible dipolar resonance structure with a carbene-type linkage of the ketenyl ligand to the tungsten centre [23]. This is expected to shorten the tungsten carbon bond, as is indeed observed in the molecular structures of **8** and **19**. It may also well be the reason for the unusual chemical shift of the tungsten-bound ketenyl carbon in **8**. Unfortunately, no $^{13}$C-NMR data were reported for **19** which would substantiate this proposal.

### 2.3. Theoretical calculations

There are two major objectives in this section, namely to rationalise the bonding of the 'four-electron-donor' nitriles in complex **8** described above and in some of the examples from the literature, comparing it with the bonding in the two-electron-donor nitrile complexes, and to trace the origin of the preference in **8** for a four-electron nitrile instead of a four-electron ketenyl [24]. These studies are based on extended Hückel calculations [25]. A complete optimisation of the geometry of a model of complex **8** was performed using density function theory (DFT) calculations [26] (ADF program [27]).

Structural data are available for a group of complexes containing side-on bound nitriles (Table 1). The simplest, most symmetric, complex with a side-on nitrile considered a 'four-electron donor' is [*mer*-$W(PMe_3)_3Cl_2(NCMe)$], (**11**), where tungsten exhibits an approximately octahedral coordination. The frontier orbitals of linear and bent NCH, as well as those of bent NCMe are shown in Scheme 1 in a three-dimensional CACAO representation [28].

When the nitrile is linear, it is a bad π-acceptor, both because the energy of the degenerate LUMOs ($\pi_{\perp}^{*}$ and $\pi_{\parallel}^{*}$) is relatively high, and, more importantly, because its largest localisation is on the less electronegative carbon atom, rather than on the nitrogen. The bending of the nitrile allows mixing between $\sigma$ and $\pi_{\parallel}$, reorienting them in such a way that a better overlap with metal orbitals can be achieved, if side-on coordination is considered. The ligand becomes both a better donor and a better acceptor. The frontier orbitals include the former lone pair $\sigma$ (6a′), the two $\pi$ orbitals, known as $\pi_{\perp}$ (2a″) and $\pi_{\parallel}$ (5a′), and two empty $\pi^*$ orbitals, known as $\pi_{\parallel}^{*}$ (7a′) and $\pi_{\perp}^{*}$ (3a″). Side-on coordination allows for an efficient back-donation, owing to the good overlap and the lower energy of the LUMO. On the other hand, bending the nitrile is an energy consuming distortion, so that only for electron rich metal centres, where back-donation is important, does this process become favourable.

The interaction diagram between the $W(PH_3)_3Cl_2$ fragment and NCH is shown in Fig. 4.

The bonding can be described by donation of electrons from 6a′ (HOMO) and also from 2a″ to two empty d orbitals of tungsten. There is some mixing with 5a′, providing a better metal–ligand overlap. This scheme agrees with our classification of the nitrile as a four-electron donor, as there are two bonding donation components involving orbitals with different symmetry. On the other hand, back donation occurs from $W(PH_3)_3Cl_2$ 1a and 2a to the two $\pi^*$ orbitals. We can measure the amount of donation and back donation by looking at the occupation of the five orbitals of the nitrile that participate in binding to the metal. The initially occupied orbitals (two electrons) become less populated in the complex (6a′ 1.846, 2a″ 1.879, 5a′ 1.928), while the initially empty ones have gained electrons (7a′ 1.057, 3a″

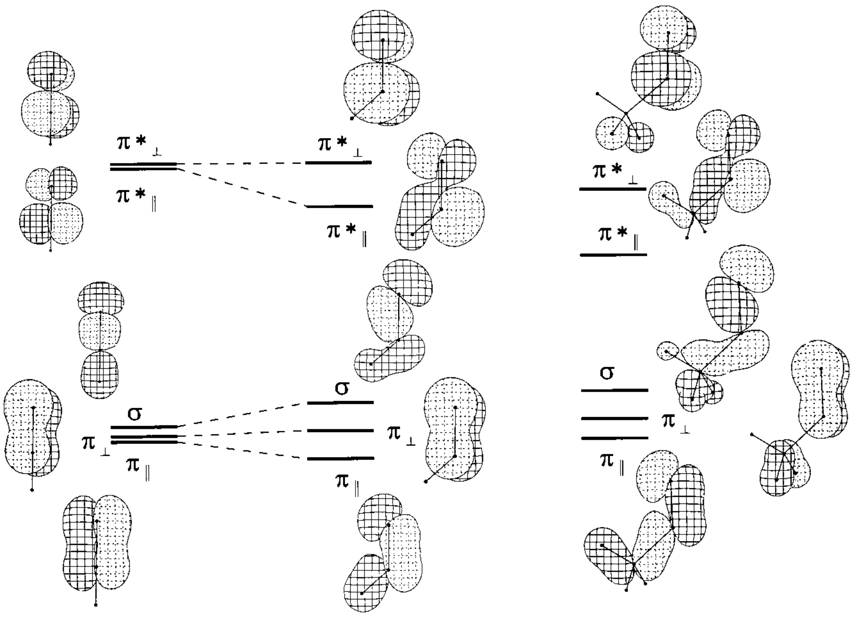

Scheme 1.

0.482). In this system, both components of the bonding help to weaken the N–C bond, which in complex **11** is indeed quite long compared with that of the free nitrile (see Table 1).

The bonding in $[(C_5Me_5)(CO)(NCMe)W\{C(SiPh_3)=C=O\}]$ (**8**) is not so easy to understand, owing to the total lack of symmetry and mixing between all the orbitals. It has been modelled for the extended Hückel calculations by $[W(C_5H_5)(CO)(H_3SiCCO)(NCMe)]$. The interaction diagram between the metal fragment and NCMe, shown in Fig. 5, is qualitatively similar to the previous one, but mixing makes interpretation more difficult. The electron occupations of the nitrile are 5a′ 1.935, 2a″ 1.875, 6a′ (HOMO) 1.894, 7a′ (LUMO) 1.012, 3a″ 0.020 electrons, suggesting by comparison with $[W(PH_3)_3Cl_2(NCH)]$ that two orbitals of the nitrile are donating electrons and that the nitrile acts as a four-electron donor. Two donation components are present, from 2a″ and 6a′ to 3a and 4a, but there is only significant back-donation to one orbital, the nitrile LUMO, 7a′. The HOMO of the metal fragment does not have the right symmetry to interact with 3a″.

Other complexes with side-on bound nitrile ligands were examined, both four-electron donors and two-electron donors. The geometry of the NCH model nitrile was kept constant, to facilitate comparisons across the series. The occupations of the five relevant levels of the nitrile after binding to the metal centres are compiled in Table 2. The two-electron-donor nitrile is characterised by involvement of only the HOMO 6a′ in bonding to the metal, the participation of 2a″ being negligible. The N–C bond is longer in the four-electron-donor nitrile species because more electrons are lost from bonding orbitals (from two instead of one), and back-donation is comparable. We add in the table the corresponding data for the related alkyne complex $[W(C_5H_5)(CO)(HCCO)(HCCH)]$, a model for $[(C_5H_5)(CO)(Et_3NC{\equiv}CMe)W\{C(p\text{-tolyl})CO\}]$ (**19**) [23], where the two HOMOs donate electrons and the alkyne is a four-electron-donor. The proposed three-electron-donor complex **15** appears, from the orbital occupations (Table 2), to have two nitrile orbitals donating electrons to the metal, but back-donation from the metal is small. Therefore, N–C bonds are not so weak and the N–C bond distance is in the range of those observed for two-electron-donor nitriles.

The second aspect concerns $[(C_5Me_5)(CO)(NCMe)W\{C(SiPh_3)=C=O\}]$ (**8**) and why the four electron donor is the nitrile and not the ketenyl anion, as might be expected, and as indeed happens for other compounds, such as $[tpb'(CO)(NCCH_3)Mo\{C(C_6H_4Me\text{-}4)CO\}]$ (**7b**). In order to trace this preference, we performed both EH and DFT calculations. The bonding of a side-on nitrile to the metal fragment was described above. Decomposition of the model complex $[W(C_5H_5)(CO)(\eta^1\text{-}H_3SiCCO)(\eta^2\text{-}NCMe)]$ molecule into different fragments, such as $[W(C_5H_5)(CO)(NCMe)]^+$ and $(H_3SiC=C=O)^-$, and comparison with the alternative $[W(C_5H_5)(CO)(\eta^2\text{-}H_3SiCCO)(\eta^1\text{-}NCMe)]$ employing similar decompositions is a helpful procedure. Both $\eta^1$-NCMe (end on) and $\eta^1\text{-}(H_3SiC=C=O)^-$ are only $\sigma$ donors, but the ketenyl forms stronger bonds. The overlap populations between the relevant fragment molecular orbitals are 0.23 for the ketenyl and 0.19 for

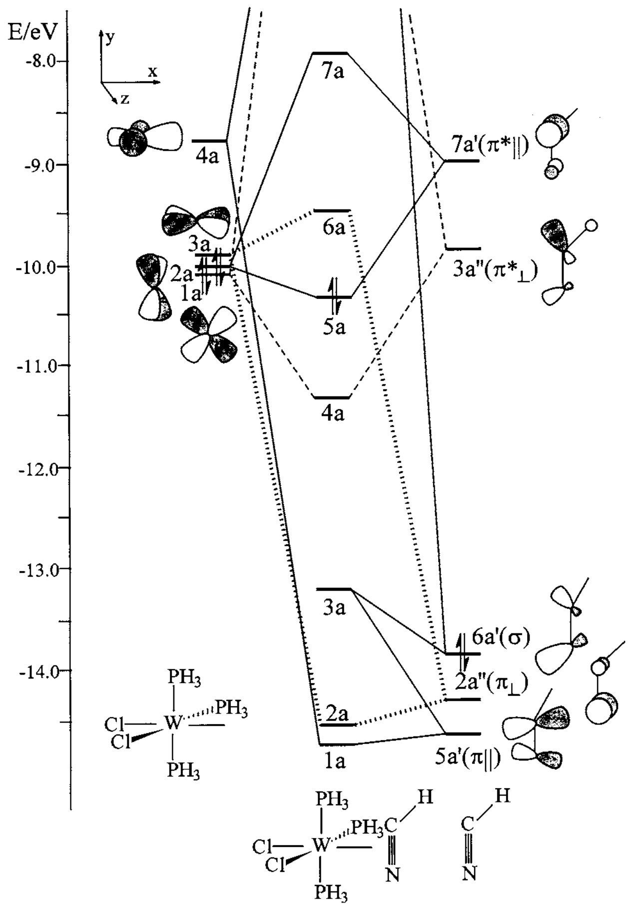

Fig. 4. Molecular orbital diagram for the interaction between $[W(PMe_3)_3Cl_2]$ and NCH.

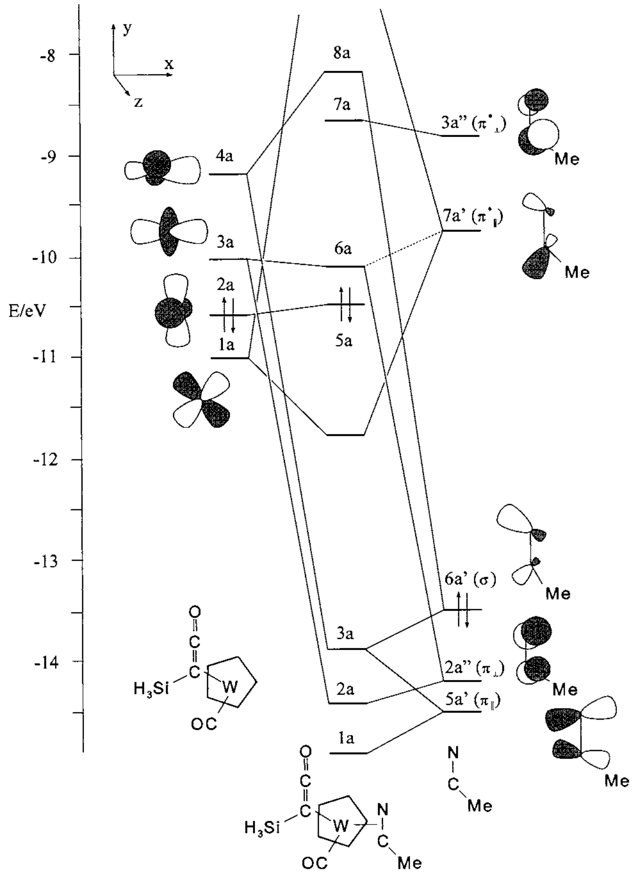

Fig. 5. Molecular orbital diagram for the interaction between $[(C_5H_5)(CO)W\{C(SiH_3)=C=O\}]$ and NCMe.

the nitrile. One reason for these values is the better energy match between interacting orbitals in the case of the ketene, thus remaining $\eta^1$ bonded in complex **8**. $\eta^2$-NCMe and $\eta^2$-$H_3SiCCO$ are both good donors and good π-acceptors.

The structure of the model compound $W(C_5H_5)$-(CO)(HCCO)(NCH) was fully optimised using DFT calculations. The final geometry is shown in Fig. 6, in two different views. The agreement between the calculated and the observed structure is quite good, especially considering that the model is significantly less bulky.

Some distances and angles can be compared. For instance, the W–N distances (Å) are 2.020 and *2.106* (calculated values in italics), W–C(nitrile) 2.058 and *2.107*, C–N 1.257 and *1.248*, W–C(CO) 1.942 and *1.936*, C–O 1.165 and *1.171*, W–C(ketenyl) 2.174 and *2.123*, W–C′(ketenyl) 2.809 and *2.794*, C–C′(ketenyl) 1.298 and *1.315*, C–O(ketenyl), 1.180 and *1.176*, while some relevant angles (°) are the following: N–C–C/H 136.1 and *135.6*, W–C–O 174.7 and *175.9*, C=C′=O 178.5 and *177.4*.

This lowest-energy structure is very similar to the X-ray-determined structure of complex **8**, showing the coordination preferences of the ligands to be determined by electronic factors.

We performed a similar geometry optimisation constraining the nitrile ligand to stay coordinated through the N atom. The final energy is 0.66 eV higher than for the previous calculation, showing that it is a local minimum.

Each of the two molecules $W(\eta^5\text{-}C_5H_5)(CO)(\eta^1\text{-}HCCO)(\eta^2\text{-}NCH)$ (**A**) and $W(\eta^5\text{-}C_5H_5)(CO)(\eta^2\text{-}HCCO)(\eta^1\text{-}NCH)$ (**B**) was decomposed into three fragments, respectively $W(\eta^5\text{-}C_5H_5)(CO)$, the nitrile and the ketenyl. The bonding energy of each molecule calcu-

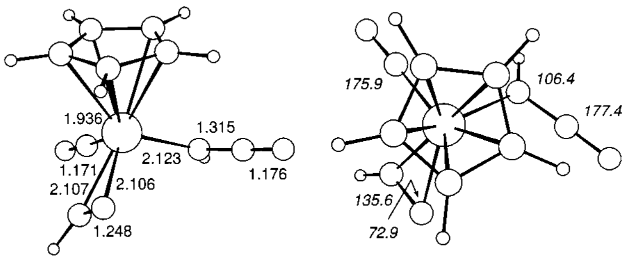

Fig. 6. DFT optimised geometry of $[(C_5H_5)(CO)W(NCH)(HC=C=O)]$, in a side view (left) and a top view (right). Bond distances (Å) are given in normal typeface, angles (°) in italics.

Table 2
Occupation of the frontier orbitals of side-on bound nitrile in several model complexes

| Complex | Model for complex | 3a″ | 7a′ | 6a′ | 2a″ | 5a′ |
|---|---|---|---|---|---|---|
| Four-electron donors | | | | | | |
| $[W(C_5H_5)(CO)(NCH)\{C(H)CO\}]$ | **8** | 0.020 | 1.012 | 1.894 | 1.875 | 1.935 |
| $[Mo(PH_3)_4Cl(HCN)]^+$ | **9** | 0.347 | 1.008 | 1.840 | 1.866 | 1.925 |
| $[W(PH_3)_3Cl_2(HCN)]$ | **11** | 0.482 | 1.057 | 1.846 | 1.879 | 1.928 |
| Three-electron donors | | | | | | |
| [Nb(tpb′)(CO)(HCCH)(HCN)] | **15** | 0.030 | 0.683 | 1.803 | 1.878 | 1.905 |
| Two-electron donors | | | | | | |
| $[Mo(C_5H_5)_2(HCN)]$ | **16** | 0.017 | 0.620 | 1.853 | 1.963 | 1.936 |
| $[Ir(C_5H_5)(PH_3)(HCN)]$ | **17** | 0.059 | 0.904 | 1.833 | 1.996 | 1.890 |
| Four-electron donor (alkyne) | | | | | | |
| $[W(C_5H_5)(CO)(HCCH)\{C(H)CO\}]$ | **19** | 0.030 | 0.866 | 1.764 | 1.750 | 1.935 |

lated relative to that of the fragments was −7.97 eV for **A** and −6.86 eV for **B**. The bonding energy can be decomposed into several terms. Among the most important we can identify the Pauli repulsion, which amounts to 23.23 eV for **A** and 17.26 eV for **B**. This term is compensated both by the stronger electrostatic interaction in **A** (−13.66 vs. −9.22 eV) and the more favourable orbital interactions in **A** (−17.64 vs. −15.13 eV). We can therefore assign the most stable geometry to stronger electrostatic and covalent interactions, in spite of a larger repulsion between closed shells.

## 3. Experimental

### *3.1. General procedures*

All operations were carried out under an atmosphere of purified argon (BASF R3-11 catalyst) using Schlenk techniques. Solvents were dried by conventional methods. The compounds $[(CO)_5Mo\{C(OMe)C_6H_4Me\text{-}4\}]$ [29], $[tpb'(CO)_2WCC_6H_4Me\text{-}4]$ (**6**) [8] and $[Br(CO)_4WCSiPh_3]$ [30] were prepared as described in the literature. NMR spectra were obtained on a Bruker AC-200 instrument (200.1 MHz for $^1H$, 50.3 MHz for $^{13}C$). $^1H$ and $^{13}C$ chemical shifts are reported versus $SiMe_4$ and were determined by reference to internal $SiMe_4$ or residual solvent peaks. The assignment of the $^{13}C$ resonances was corroborated by DEPT spectra. IR spectra were measured with a Bruker IFS-28 Fourier transform spectrometer in $CaF_2$ cells.

### *3.2. Preparation of [tpb′(CO)$_2$MoCC$_6$H$_4$Me-4] (**4b**)*

A 3.0 g (12.0 mmol) sample of $BBr_3$ was slowly added to a cold (−15°C) suspension of 3.28 g (8.9 mmol) $[(CO)_5Mo\{C(OMe)C_6H_4Me\text{-}4\}]$ in 125 ml of cold pentane. The mixture was stirred vigorously at −20°C for 80 min and then cooled to −80°C. The supernatant was removed and the residue suspended in cold (−40°C) $CH_2Cl_2$. Solid Ktpb′ (3.0 g, 8.9 mmol) was added and the mixture was stirred at −20°C for 36 h. After removal of solvent under reduced pressure, the dark-yellow residue was chromatographed two times at r.t. on $Al_2O_3$ with 4:1 *n*-hexane–$CH_2Cl_2$ as the mobile phase. The product was obtained from the orange–yellow fraction after removal of solvent under reduced pressure. Recrystallisation from MeCN at 4°C affords orange–yellow crystals of **4b**·MeCN (2.8 g, 57%). IR (in THF) $\nu_{CO}$ (cm$^{-1}$): 1982(m), 1899(s) — $^1H$-NMR (in $CDCl_3$): $\delta$ 2.32 (s, 3H, Me-4), 2.34 (s, 3H, tpb′–$CH_3$), 2.36 (s, 6H, tpb′–$CH_3$), 2.41 (s, 3H, tpb′–$CH_3$), 2.49 (s, 6H, tpb′–$CH_3$), 5.74 (s, 1H, tpb′–CH), 5.83 (s, 2H, tpb′–CH), 7.09 and 7.44 [$(AB)_2$-system, $^3J_{HH} = 8.1$ Hz, 4H, $C_6H_4$) — $^{13}C\{^1H\}$-NMR (in $CDCl_3$): $\delta$ 12.6, 12.7, 14.6, 15.8 (tpb′–$CH_3$), 21.6 (Me-4), 106.1, 106.2 (tpb′–CH), 128.8, 129.1 ($C_6H_4$), 138.6, 143.8, 144.4, 144.8, 151.1, 151.2, (tpb′–*C*$CH_3$, $C_6H_4$–C-1, C-4), 225.8 (CO); 288.9 (carbyne-C) — $^{11}B\{^1H\}$-NMR ($CDCl_3$): $\delta$ −8.8 — MS: *m*/*z* (relative intensity) 554 (8, $M^+$), 526 (36, $[M-CO]^+$), 498 (100, $[M-2CO]^+$).

### *3.3. Preparation of [(C$_5$Me$_5$)(CO)$_2$WCSiPh$_3$] (**5**)*

Complex **5** was prepared from 3 g (4.6 mmol) of $[Br(CO)_4WCSiPh_3]$ and 1.2 g (6.9 mmol) of $K(C_5Me_5)$ following the procedure described for the $C_5H_5$ derivative in Ref. [30]. Yield, 880 mg (30%) orange microcrystals. IR (in $CH_2Cl_2$) $\nu_{CO}$ (cm$^{-1}$): 1987 (s), 1909 (vs) — $^1H$-NMR (in $CD_2Cl_2$): $\delta$ 2.13 (s, 15H, $C_5Me_5$), 7.48 (m, 15H, $SiPh_3$) — $^{13}C\{^1H\}$-NMR (in $CD_2Cl_2$): $\delta$ 11.3 ($C_5$*Me*$_5$), 105.7 (*C*$_5$Me$_5$), 128.1, 129.7, 135.2, 136.0 (Ph), 227.5 (CO), 355.1 (carbyne-C) — MS: *m*/*z* (relative intensity) 646 (46, $M^+$), 618 (36, $[M-CO]^+$), 590 (100, $[M-2CO]^+$).

### 3.4. Preparation of [tpb′(CO)(NCMe)Mo{C($C_6H_4$Me-4)CO}] (**7b**)

A 200 mg (0.4 mmol) sample of **4b** was dissolved in the minimum amount of acetonitrile at 60°C. The dark solution was allowed to stand in the daylight at r.t. for 2 days. Upon cooling to 0°C most of the unreacted **4b** crystallises. The more soluble product **7b** (60 mg, 28%) is separated as blue–green crystals from residual orange–red **4b** by fractional crystallisation of the dark-green supernatant at −20°C. IR (in THF) $\nu_{CO}$ ($cm^{-1}$): 1887(vs), 1773(m, br) — $^1$H-NMR (in $CD_2Cl_2$): δ 1.30, 1.51, 2.28, 2.35, 2.40, 2.48, 2.53, 2.73 (each s, 3H; tpb′–$CH_3$, $CH_3CN$ and tolyl-$CH_3$), 5.67 (s, 1H, tpb′–CH), 5.80 (s, 1H, tpb′–CH), 5.95 (s, 1H, tpb′–CH), 6.82 and 7.03 [$(AB)_2$-system, $^3J_{HH} = 7.9$ Hz, 4H, $C_6H_4$) — $^{13}C\{^1H\}$-NMR (in $CD_2Cl_2$): δ 5.1 ($\mathit{C}H_3CN$), 12.8, 13.1, 13.7, 15.2 (tpb′–$CH_3$), 21.6 (Me-4), 106.4, 106.8 (tpb′–CH), 125.9, 129.3 ($C_6H_4$), 137.7, 138.3 ($C_6H_4$–C-1, C-4), 142.7 ($CH_3\mathit{C}N$), 144.9, 145.7, 145.9, 150.6, 151.3, 154.0 (tpb′–$\mathit{C}CH_3$), 209.0 (C=*C*=O), 231.3 (CO), 231.6 (*C*=C=O) — $^{11}B\{^1H\}$-NMR ($CD_2Cl_2$): δ −8.1 — MS: m/z (relative intensity) 554 (10, $[M-CH_3CN]^+$), 526 (38, $[M-CH_3CN–CO]^+$), 498 (100, $[M-CH_3CN–2CO]^+$), 297 (56, $[tpb′]^+$), 28 (57, CO).

### 3.5. Preparation of [($C_5Me_5$)(CO)(NCMe)W{C($SiPh_3$)CO}] (**8**)

A 120 mg (0.19 mmol) sample of **5** was added to 10 ml of cold (−20°C) acetonitrile. The stirred mixture is slowly warmed to r.t. After 2 h the volume of the solution was reduced to 3 ml under reduced pressure. The product **8** (55 mg, 42%) precipitated from the green solution at −25°C as dark blue crystals. The mother liquor mainly contained complex **5**. IR (in $CH_2Cl_2$) $\nu_{CO}$ ($cm^{-1}$): 2024(s), 1887(s); $\nu_{CN}$ ($cm^{-1}$): 2073(w) — $^1$H-NMR (in $CD_2Cl_2$): δ 1.83 (s, 15H, $C_5Me_5$), 2.95 (s, 3H, $NCCH_3$), 7.46 (m, 15H,$SiPh_3$) — $^{13}C\{^1H\}$-NMR (in $CD_2Cl_2$): δ 10.2 ($C_5\mathit{Me}_5$), 18.8 ($NC\mathit{C}H_3$), 20.7 (*C*=C=O), 109.6 ($\mathit{C}_5Me_5$), 128.1, 129.6, 136.2, 137.1 (Ph), 169.3 (C=*C*=O), 203.4 ($N\mathit{C}CH_3$), 232.9 (CO) — MS: m/z (relative intensity) 646 (48, $[M-CH_3CN]^+$), 618 (38, $[M-CH_3CN–CO]^+$), 590 (100, $[M-CH_3CN–2CO]^+$) — Anal. Calc. for $C_{33}H_{33}NO_2SiW$ (687.57): C, 57.64; H, 4.83; N, 2.03. Found: C, 57.13; H, 5.14; N, 2.91.

### 3.6. X-ray crystal structure determination of [tpb′$(CO)_2$M≡$CC_6H_4$Me-4] (M = Mo, **4b**), (M = W, **6**), [tpb′(CO)($NCCH_3$)Mo{C($C_6H_4$Me-4)CO}] (**7b**) and [($C_5Me_5$)(CO)(NCMe)W{C($SiPh_3$)CO}] (**8**)

Intensity data were collected with Syntex R3 (complex **4b**) and Siemens–Stoe AED2 four-circle diffractometers (complexes **6**, **7b** and **8**) and corrected for Lorentz, polarisation and absorption effects (Tables 3 and 4). The structures were solved by the heavy atom or direct methods and refined on $F^2$ by full-matrix least-squares using all measured unique reflections. All non-hydrogen atoms were given anisotropic thermal parameters.

Table 3
Details of the crystal structure determinations of the complexes [tpb′$(CO)_2MCC_6H_4$Me-4] (**4b**) (M = Mo) and (**6**) (M = W)

| | **4b** | **6** |
|---|---|---|
| Crystal system | Monoclinic | Monoclinic |
| Space group | $P2_1/c$ | $P2_1/c$ |
| Unit cell dimensions | | |
| a (Å) | 10.740(2) | 10.639(5) |
| b (Å) | 14.307(3) | 14.244(7) |
| c (Å) | 19.363(4) | 19.286(10) |
| β (°) | 103.11(2) | 102.78(4) |
| V ($Å^3$) | 2897.7 | 2850.2 |
| Z | 4 | 4 |
| $D_{calc.}$ (g $cm^{-3}$) | 1.360 | 1.588 |
| F(000) | 1224 | 1352 |
| μ (Mo–$K_\alpha$) ($mm^{-1}$) | 0.49 | 4.09 |
| X-Radiation, λ (Å) | Mo–$K_\alpha$, graphite monochromated, 0.71069 | |
| Data collection temperature (K) | Ambient | 203 |
| $2\vartheta_{max}$ (°) | 50 | 58 |
| hkl-Range | 0/12, 0/17, −23/22 | −14/14, 0/19, 0/26 |
| Reflections measured | 5373 | 7892 |
| Unique | 5126 | 7591 |
| Observed [$I \geq 2\sigma(I)$] | 3980 | 6653 |
| Absorption correction | Empirical | Empirical |
| Parameters refined | 361 | 360 |
| GOF | 1.112 | 1.049 |
| R (observed reflections only) | 0.041 | 0.028 |
| $wR_2$ (all reflections) [a] | 0.094 | 0.075 |

[a] $w = 1/[\sigma^2(F_o^2)+(AP)^2+BP]$, $P = \max(F_o^2, 0)+2F_c^2)/3$, where A = 0.0338 and 0.043 for **4b** and **6**, respectively, and B = 1.78 and 2.42 for **4b** and **6**, respectively.

The hydrogen atoms on boron were located from difference Fourier maps and refined with isotropic atomic displacement parameters. All other hydrogen atoms were input in calculated positions.

The calculations were performed using the programs SHELXS-86 [31] and SHELXL-93 [32]. Graphical representations were drawn with the SCHAKAL-88 program [33].

### 3.7. Molecular orbital calculations

Extended Hückel calculations were performed using the extended Hückel method [25] with modified $H_{ij}$ values [34]. The basis set for the metal atoms consisted of *n*s, *n*p and (*n-1*)d orbitals. The s and p orbitals were described by single Slater-type wave functions, and the d orbitals were taken as contracted linear combinations of two Slater-type wave functions. Only s and p orbitals were considered for Cl. The parameters used for W were ($H_{ii}$ (eV), $\zeta$): 6s −8.26, 2.341; 6p −5.17, 2.309; 5d −10.37, 4.982, 2.068 (2), 0.6685 (C1), 0.5424 (C2); for Cl: ($H_{ii}$ (eV), z): 3s −30.00, 2.033; 3p −15.00, 2.033. Standard parameters were used for other atoms. Interaction diagrams were drawn using the program CACAO [28].

The calculations were performed on model complexes with idealised geometries. NCH was used as the nitrile ligand, with bond distances C–N, 1.27, C–H, 1.03 Å and the N–C–H angle set to 129°. Substituents on other ligands ($CH_3$, Ph, $SiPh_3$) were replaced by hydrogen. Dmpe was approximated by two $Ph_3$ ligands. The geometry of **9** and **11** was forced to regular octahedral, with the bond distances taken from the real structures.

The model for complex **8** has approximately a piano stool geometry with a $C_5H_5$–W–C(carbonyl) angle of 118°, a $C_5H_5$–W–C(ketenyl) angle of 115° and a $C_5H_5$–W–C(nitrile) angle of 122°. Bond distances for the ketenyl, the carbonyl and the $C_5H_5$ ligand were taken from the structure.

Table 4
Details of the crystal structure determinations of the complexes [tpb′(CO)(NCMe)Mo {C($C_6H_4$Me-4)CO}] (**7b**) and [($C_5Me_5$)(CO)-(NCMe)W{C($SiPh_3$)CO}] (**8**)

| | **7b** | **8** |
|---|---|---|
| Crystal system | Triclinic | Triclinic |
| Space group | $P\bar{1}$ | $P\bar{1}$ |
| Unit cell dimensions | | |
| *a* (Å) | 10.145(7) | 10.123(5) |
| *b* (Å) | 10.441(8) | 12.172(6) |
| *c* (Å) | 15.729(12) | 13.808(7) |
| $\alpha$ (°) | 109.10(6) | 64.16(3) |
| $\beta$ (°) | 93.87(6) | 85.00(3) |
| $\lambda$ (°) | 91.16(6) | 69.88(3) |
| *V* (Å$^3$) | 1569.2 | 1433.9 |
| *Z* | 2 | 2 |
| $D_{calc.}$ (g cm$^{-3}$) | 1.343 | 1.592 |
| *F*(000) | 656 | 684 |
| $\mu$(Mo–K$_\alpha$) (mm$^{-1}$) | 0.46 | 4.10 |
| X-radiation, $\lambda$ (Å) | Mo–K$_\alpha$, graphite monochromated, 0.71069 | |
| Data collection temperature (K) | 203 | 203 |
| $2\vartheta_{max}$ (°) | 52 | 50 |
| *hkl*-range | −12/10, −12/12, 0/19 | −11/12, −12/14, 0/16 |
| Reflections measured | 6000 | 5053 |
| Unique | 6000 | 5043 |
| Observed [$I \geq 2\sigma(I)$] | 5187 | 4724 |
| Absorption correction | Empirical | Empirical |
| Parameters refined | 389 | 352 |
| GOF | 1.077 | 1.040 |
| *R* (observed reflections only) | 0.062 | 0.022 |
| $wR_2$ (all reflections) [a] | 0.183 | 0.057 |

[a] $w = 1/[\sigma^2(F_o^2)+(AP)^2+BP]$, $P = \max(F_o^2, 0)+2F_c^2)/3$, where $A = 0.1332$ and 0.0392 for **7b** and **8**, respectively, and $B = 0.58$ and 0.55 for **7b** and **8**, respectively.

The iridium compound **17** was modelled by a two-legged piano stool with $C_5H_5$–Ir–L angles of 135°, respectively. Bond distances of the ($C_5H_5$)Ir moiety and the Ir–L distances were taken from the structure of **17**.

DFT calculations [26] were carried out using the Amsterdam Density Functional (ADF) program [27] developed by Baerends and co-workers [35]. Vosko, Wilk and Nusair's local exchange correlation potential was used [36], with Becke's nonlocal exchange and Perdew's correlation corrections [37]. The geometry optimisation procedure was based on the method developed by Versluis and Ziegler [38], using the non-local correction terms in the calculation of the gradients. A full geometry optimisation of the model compound [W($C_5H_5$)(CO)(HCCO)(NCH)] was performed, starting from an idealised geometry, based on the X-ray determined structure, where both the nitrile and the ketene were half way between $\eta^1$ and $\eta^2$. The relativistic effects were treated by a quasi-relativistic method where Darwin and mass–velocity terms are incorporated [39]. The core orbitals were frozen for W ([1–5]s, [2–5]p, [3–4]d) and C, N, O (1s). Triple-$\zeta$ Slater-type orbitals (STO) were used for H 1s, C, N, O 2s and 2p, W 6s and 6p. A set of polarisation functions was added: H (single $\zeta$, 2p), C, N, O (single $\zeta$, 3d).

## 4. Supplementary material

Crystallographic data (excluding structure factors) for the structures reported in this paper have been deposited with the Cambridge Crystallographic Data Centre as supplementary publication nos. CCDC-132488 (**4b**), -132489 (**6**), -132490 (**7b**) and -132491 (**8**). Copies of the data can be obtained free of charge on application to The Director, CCDC, 12 Union Road, Cambridge CB2 1EZ, UK (Fax: +44-1223-336-033; e-mail: deposit@ccdc.cam.ac.uk or www: http://www.ccdc.cam.ac.uk).

## Acknowledgements

This work was supported by the Deutsche Forschungsgemeinschaft under the auspices of the Sonderforschungsbereich 247 of the Universität Heidelberg and by the Fonds der Chemischen Industrie. The authors thank the Deutscher Akademischer Austauschdienst and the Conselho de Reitores das Universidades Portuguesas for a scientific exchange grant within the Acções Integradas Luso-Alemãs scheme. A Heisenberg fellowship to H.W. is gratefully acknowledged.

## References

[1] F.R. Kreißl, A. Frank, U. Schubert, T.L. Lindner, G. Huttner, Angew. Chem. 88 (1976) 649.

[2] (a) F.R. Kreißl, K. Eberl, W. Uedelhoven, Chem. Ber. 110 (1977) 3782. (b) W.J. Sieber, M. Wolfgruber, N.H. Tran-Huy, H.R. Schmidt, H. Heiss, P. Hofmann, F.R. Kreißl, J. Organomet. Chem. 340 (1988) 341. (c) W. Uedelhoven, K. Eberl, F.R. Kreißl, Chem. Ber. 112 (1979) 3376.

[3] (a) H.P. Kim, R.J. Angelici, Adv. Organomet. Chem. 27 (1987) 51. (b) A. Mayr, C.M. Bastos, Progr. Inorg. Chem. 40 (1992) 1, and references cited therein. (c) P.F. Engel, M. Pfeffer, Chem. Rev. 95 (1995) 2281 and references cited therein.

[4] F.R. Kreissl, in: H. Fischer, P. Hofmann, F.R. Kreissl, R.R. Schrock, U. Schubert, K. Weiss (Eds.), Carbyne Complexes, VCH, Weinheim, 1988, pp. 99–146.

[5] G.L. Geoffroy, S.L. Bassner, Adv. Organomet. Chem. 28 (1988) 1.

[6] (a) H. Wadepohl, G.P. Elliott, H. Pritzkow, F.G.A. Stone, A. Wolf, J. Organomet. Chem. 482 (1994) 243. (b) H. Wadepohl, U. Arnold, H. Pritzkow, Angew. Chem. 109 (1997) 1009. (c) H. Wadepohl, U. Arnold, H. Pritzkow, A. Wolf, in: W. Siebert (Ed.), Advances in Boron Chemistry, Special Publication No. 201, The Royal Society of Chemistry, Cambridge 1997, pp. 385–388.

[7] T. Desmond, F.J. Lalor, G. Ferguson, M. Parvez, J. Am. Chem. Soc. 107 (1985) 4474.

[8] J.C. Jeffery, F.G.A. Stone, G.K. Williams, Polyhedron 10 (1991) 215.

[9] D.C. Brower, M. Stoll, J.L. Templeton, Organometallics 8 (1989) 2786.

[10] (a) M. Green, J.A.K. Howard, A.P. James, A.N. de M. Jelfs, C.M. Nunn, F.G.A. Stone, J. Chem. Soc. Chem. Commun. (1984) 1623. (b) M. Green, J.A.K. Howard, A.P. James, C.M. Nunn, F.G.A. Stone, J. Chem. Soc. Dalton Trans. (1986) 187.

[11] A.F. Hill, J.M. Malget, A.J.P. White, D.J. Williams, J. Chem. Soc. Chem. Commun. (1996) 721.

[12] U. Schubert, in Ref. [4], p. 39–58.

[13] L. Karakida, T. Fukuyama, K. Kuchitsu, Bull. Chem. Soc. Jpn. 47 (1974) 299.

[14] Acetonitrile is often found as a solvent of crystallisation in organometallic crystals. A statistical analysis of the NC bond length and NCC angle in such structures in the Cambridge Crystallographic Database gave sharp distributions centred in the range 1.10–1.15 Å and 174–180°, respectively.

[15] K.R. Birdwhistell, T.L. Tonker, J.L. Templeton, J. Am. Chem. Soc. 107 (1985) 4474.

[16] F.R. Kreißl, P. Friedrich, G. Huttner, Angew. Chem. 89 (1977) 110.

[17] E.O. Fischer, A.C. Filippou, H.G. Alt, K. Ackermann, J. Organomet. Chem. 254 (1983) C21.

[18] A.K. List, G.L. Hillhouse, A.L. Rheingold, J. Am. Chem. Soc. 110 (1988) 4855.

[19] A.P. Cox, L.F. Thomas, J. Sheridan, Spectrochim. Acta 15 (1959) 542.

[20] D.C. Brower, K.R. Birdwhistell, J.L. Templeton, Organometallics 5 (1986) 94.

[21] (a) V.G. Albano, D. Braga, P. Chini, S. Martinengo, D. Strumolo, Eur. Cryst. Meeting 6 (1980) 71. (b) T.C. Wright, G. Wilkinson, M. Motevalli, M.B. Hursthouse, J. Chem. Soc. Dalton Trans. (1986) 2017. (c) P.A. Chetcuti, C.B. Knobler, M.F. Hawthorne, Organometallics 5 (1986) 1913. (d) P.A. Chetcuti, C.B. Knobler, M.F. Hawthorne, Organometallics 7 (1988) 650. (e) S.J. Anderson, F.J. Wells, G. Wilkinson, B. Hussain, M.B. Hursthouse, Polyhedron 7 (1988) 2615. (f) J. Barrera, M. Sabat, W.D. Harman, J. Am. Chem. Soc. 113 (1991) 8178. (g) J. Barrera, M. Sabat, W.D. Harman, Organometallics 12 (1993) 4381. (h) S. Thomas, E.R.T. Tiekink, C.G. Young, Organometallics 15 (1996) 2428. (i) P. Lorente, C. Carfagna, M. Etienne, B. Donnadieu, Organometallics 15 (1996) 1090. (j) J.L. Kiplinger, A.M. Ariff, T.G. Richmond, Organometallics 16 (1997) 246. (k) S. Thomas, C.G. Young, E.R.T. Tiekink, Organometallics 17 (1998) 182.

[22] (a) J.L. Templeton, B.C. Ward, J. Am. Chem. Soc. 102 (1980) 3288. (b) J.L. Templeton, Adv. Organomet. Chem. 29 (1989) 1. (c) K. Tatsumi, R. Hoffmann, J.L. Templeton, Inorg. Chem. 21 (1982) 466.

[23] F.R. Kreißl, G. Reber, G. Müller, Angew. Chem. 98 (1986) 640.

[24] For electron bookeeping purposes a side-on coordinated ketenyl is a four-electron ligand if considered monoanionic, or a three-electron ligand if taken as neutral.

[25] (a) R. Hoffmann, J. Chem. Phys. 39 (1963) 1397. (b) R. Hoffmann, W.N. Lipscomb, J. Chem. Phys. 36 (1962) 2179.

[26] R.G. Parr, W. Yang, Density Functional Theory of Atoms and Molecules, Oxford University Press, New York, 1989.

[27] Amsterdam Density Functional (ADF) program, release 2.2, Vrije Universiteit, Amsterdam, The Netherlands, 1995.

[28] C. Mealli, D.M. Proserpio, J. Chem. Ed. 67 (1990) 39.

[29] E.O. Fischer, A. Maasböl, Chem. Ber. 100 (1967) 2445.

[30] E.O. Fischer, H. Hollfelder, P. Friedrich, F.R. Kreißl, G. Huttner, Angew. Chem. 89 (1977) 416.

[31] G.M. Sheldrick, SHELXS-86, Universität Göttingen, 1986.

[32] G.M. Sheldrick, SHELXL-93, Universität Göttingen, 1993.

[33] E. Keller, SCHAKAL 88, A FORTRAN Program for the Graphical Representation of Molecular and Crystallographic Models, Universität Freiburg, 1988.

[34] J.H. Ammeter, H.-J. Bürgi, J.C. Thibeault, R. Hoffmann, J. Am. Chem. Soc. 100 (1978) 3686.

[35] (a) E.J. Baerends, D. Ellis, P. Ros, Chem. Phys. 2 (1973) 41. (b) E.J. Baerends, P. Ros, Int. J. Quantum Chem. S12 (1978) 169. (c) P.M. Boerrigter, G. te Velde, E.J. Baerends, Int. J. Quantum Chem. 33 (1988) 87. (d) G. te Velde, E.J. Baerends, J. Comp. Phys. 99 (1992) 84.

[36] S.H. Vosko, L. Wilk, M. Nusair, Can. J. Phys. 58 (1980) 1200.

[37] (a) A.D. Becke, J. Chem. Phys. 88 (1987) 1053. (b) A.D. Becke, J. Chem. Phys. 84 (1986) 4524. (c) J.P. Perdew, Phys. Rev. B33 (1986) 8822. (d) J.P. Perdew, Phys. Rev. B34 (1986) 7406.

[38] (a) L. Versluis, T. Ziegler, J. Chem. Phys. 88 (1988) 322. (b) L. Fan, T. Ziegler, J. Chem. Phys. 95 (1991) 7401.

[39] (a) T. Ziegler, V. Tschinke, E.J. Baerends, J.G. Snijders, W. Ravenek, J. Phys. Chem. 93 (1989) 3050. (b) J.G. Snijders, E.J. Baerends, Mol. Phys. 36 (1978) 1789. (c) J.G. Snijders, E.J. Baerends, P. Ros, Mol. Phys. 38 (1979) 1909.